Alzheimer's & Dementia: Translational Research & Clinical Interventions 5 (2019) 338-346

Featured Article

Rates of lobar atrophy in asymptomatic *MAPT* mutation carriers

Qin Chen[a,b], Bradley F. Boeve[c,d], Matthew Senjem[a], Nirubol Tosakulwong[e], Timothy G. Lesnick[e], Danielle Brushaber[d,e], Christina Dheel[c,d], Julie Fields[f], Leah Forsberg[c,d], Ralitza Gavrilova[g], Debra Gearhart[c,d], Jonathan Graff-Radford[c,d], Neill R. Graff-Radford[h], Clifford R. Jack, Jr.[a,d], David T. Jones[c,d], David S. Knopman[c,d], Walter K. Kremers[e], Maria Lapid[f], Rosa Rademakers[d,i], Jeremy Syrjanen[e], Adam L. Boxer[j], Howie Rosen[j], Zbigniew K. Wszolek[h], Kejal Kantarci[a,d,*], on Behalf of the LEFFTDS Consortium[1]

[a]*Department of Radiology, Mayo Clinic, Rochester, MN, USA*
[b]*Department of Neurology, West China Hospital of Sichuan University, Chengdu, Sichuan, China*

Boeve B. has served as an investigator for clinical trials sponsored by GE Healthcare and Axovant; he receives royalties from the publication of a book entitled Behavioral Neurology Of Dementia (Cambridge Medicine, 2009, 2017); he serves on the Scientific Advisory Board of the Tau Consortium; and he receives research support from NIH, the Mayo Clinic Dorothy, and Harry T. Mangurian Jr. Lewy Body Dementia Program and the Little Family Foundation. Senjem M. owns medical-related stocks in the following companies, unrelated to the current work: Align Technology, Inc., CRISPR Therapeutics, Ionis Pharmaceuticals, Johnson & Johnson, LHC Group, Inc., Medtronic, Inc., Mesa Laboratories, Inc., Natus Medical Inc., and Varex Imaging Corporation; he has owned medical-related stocks within the past three years in the following companies, unrelated to the current work: Gilead Sciences, Inc., Globus Medical Inc., Inovio Biomedical Corp., Oncothyreon, Inc., Parexel International Corporation. Fields J. receives research support from NIH. Forsberg L. receives research support from NIH. Gavrilova R. receives research support from NIH. Graff-Radford J. for special issue on frontotemporal lobar degeneration, receives research support from the NIH. Graff-Radford N. receives royalties from UpToDate, has participated in multicenter therapy studies by sponsored by Biogen, TauRx, AbbVie, Novartis, and Lilly. He receives research support from NIH. Jack C.R. Jr. consults for Eli Lilly and serves on an independent data monitoring board for Roche but he receives no personal compensation from any commercial entity. He receives research support from the NIH. Jones D. receives research support from NIH and the Minnesota Partnership for Biotechnology and Medical Genomics. Knopman D. serves on the DSMB of the DIAN-TU study, is a site PI for clinical trials sponsored by Biogen, Lilly, and the University of Southern California, and is funded by NIH. Kremers K.W. receives research funding from AstraZeneca, Biogen, Roche, DOD, and NIH. Rademakers R. receives research funding from NIH and the Bluefield Project to Cure Frontotemporal Dementia. Boxer A. receives research support from NIH, the Tau Research Consortium, the Association for Frontotemporal Degeneration, Bluefield Project to Cure Frontotemporal Dementia, Corticobasal Degeneration Solutions, the Alzheimer's Drug Discovery Foundation, and the Alzheimer's Association; he has served as a consultant for Aeton, Abbvie, Alector, Amgen, Arkuda, Ionis, IPierian, Janssen, Merck, Novartis, Samumed, Toyama, and UCB and received research support from Avid, Biogen, BMS, C2N, Cortice, Eli Lilly, Forum, Genentech, Janssen, Novartis, Pfizer, Roche, and TauRx. Rosen H. has received research support from Biogen Pharmaceuticals, has consulting agreements with Wave Neuroscience and Ionis Pharmaceuticals, and receives research support from NIH. Wszolek Z. is partially supported by the NIH/NIA (primary) and NIH/NINDS (secondary) 1U01AG045390-01A1, Mayo Clinic Center for Regenerative Medicine, the gift from Carl Edward Bolch, Jr., and Susan Bass Bolch, The Sol Goldman Charitable Trust, and Donald G. and Jodi P. Heeringa, and he is an PI for Mayo Clinic Florida site on therapeutic Abbvie Inc. mediation trials. Kantarci K. serves on the Data Safety Monitoring Board for Takeda Global Research & Development Center, Inc. and Data Monitoring Boards of Pfizer and Janssen Alzheimer Immunotherapy; she receives research support from the Avid Radiopharmaceuticals, Eli Lilly. She is funded by the Alzheimer's Drug Discovery Foundation and NIH. The other authors have nothing to disclose.

[1]LEFFTDS Consortium: Giovanni Coppola[1], Bradford C. Dickerson[2], Susan Dickinson[3], Kelly Faber[4], Jamie Fong[5], Tatiana Foroud[4], Nupur Ghoshal[6], Jill Goldman[7], Murray Grossman[8], Hilary W. Heuer [5], John Hsiao[9], Ging-Yuek R. Hsiung[10], Edward Huey[7], David J. Irwin[8], Anna M. Karydas[5], John Kornak[5], Joel Kramer[5], Walter A. Kukull[11], Diane Lucente[2], Codrin Lungu[12], Ian R.A. Mackenzie[10], Scott McGinnis[2], Bruce L. Miller[5], Leonard Petrucelli[13], Madeline Potter[4], Eliana M. Ramos[1], Katherine P. Rankin[5], Katya Rascovsky[8], Leslie Shaw[8], Marg Sutherland[12], Nadine Tatton[3], Joanne Taylor[5], Arthur W. Toga[14], John Trojanowski[8], Sandra Weintraub[15], Bonnie Wong[2]. [1]UCLA, Los Angeles, CA, USA; [2]Harvard University/MGH, Boston, MA, USA; [3]Association for Frontotemporal Degeneration, Radnor, PA, USA; [4]National Cell Repository for Alzheimer's Disease (NCRAD), Indiana University, Indianapolis, IN, USA; [5]UCSF, San Francisco, CA, USA; [6]Washington University, St. Louis, MO, USA; [7]Columbia University, New York, NY, USA; [8]University of Pennsylvania, Philadelphia, PA, USA; [9]National Institute on Aging (NIA), Bethesda, MD, USA; [10]University of British Columbia, Vancouver, British Columbia, Canada; [11]National Alzheimer Coordinating Center (NACC), University of Washington, Seattle, WA, USA; [12]National Institute of Neurological Disorders and Stroke (NINDS), Bethesda, MD, USA; [13]Mayo Clinic, Jacksonville, FL, USA; [14]Laboratory of Neuroimaging (LONI), USC, Los Angeles, CA, USA; [15]Northwestern University, Chicago, IL, USA.

*Corresponding author. Tel.: 507 284 9770; Fax: 507 284 9778.
E-mail address: kantarci.kejal@mayo.edu

https://doi.org/10.1016/j.trci.2019.05.010

[c]Department of Neurology, Mayo Clinic, Rochester, MN, USA
[d]Alzheimer's Disease Research Center, Mayo Clinic, Rochester, MN, USA
[e]Department of Health Sciences Research, Mayo Clinic, Rochester, MN, USA
[f]Department of Psychology and Psychiatry, Mayo Clinic, Rochester, MN, USA
[g]Department of Clinical Genomic and Neurology, Mayo Clinic, Rochester, MN, USA
[h]Department of Neurology, Mayo Clinic, Jacksonville, FL, USA
[i]Department of Neuroscience, Mayo Clinic, Jacksonville, FL, USA
[j]Memory and Aging Center, University of California San Francisco, San Francisco, CA, USA

Abstract

Introduction: The aim of this study was to investigate the rates of lobar atrophy in the asymptomatic microtubule-associated protein tau (*MAPT*) mutation carriers.

Methods: *MAPT* mutation carriers (n = 14; 10 asymptomatic, 4 converters from asymptomatic to symptomatic) and noncarriers (n = 13) underwent structural magnetic resonance imaging and were followed annually with a median of 9.2 years. Longitudinal changes in lobar atrophy were analyzed using the tensor-based morphometry with symmetric normalization algorithm.

Results: The rate of temporal lobe atrophy in asymptomatic *MAPT* mutation carriers was faster than that in noncarriers. Although the greatest rate of atrophy was observed in the temporal lobe in converters, they also had increased atrophy rates in the frontal and parietal lobes compared to noncarriers.

Discussion: Accelerated decline in temporal lobe volume occurs in asymptomatic *MAPT* mutation carriers followed by the frontal and parietal lobe in those who have become symptomatic. The findings have implications for monitoring the progression of neurodegeneration during clinical trials in asymptomatic *MAPT* mutation carriers.

Keywords: Frontotemporal dementia; Magnetic resonance image; *MAPT*; Asymptomatic; Longitudinal

1. Introduction

Frontotemporal lobar degeneration (FTLD) is a progressive clinical syndrome with several possible etiologies and with heterogeneous clinical features, including behavioral and language disorders, executive dysfunction, and impaired social cognition, while patients can also develop features of motor neuron disease, progressive supranuclear palsy or corticobasal syndrome [1]. About 30%-50% FTLD patients have an autosomal dominant pattern of inheritance [2], with many showing mutations in the microtubule-associated protein tau (*MAPT*) gene [3]. Mutations in the *MAPT* gene result in filamentous accumulation of hyperphosphorylated tau in neurons and glia leading to neurodegeneration, atrophy, white matter microstructure alterations, and metabolic changes years before the onset of clinical symptoms [3–7]. Families characterized by the presence of *MAPT* mutations can be investigated for early neurodegenerative changes and identifying biomarkers for tracking disease progression during potential disease-modifying therapies.

Structural magnetic resonance imaging (MRI) has captured disease-specific neurodegeneration in patients with mild cognitive impairment (MCI) [8,9], Alzheimer's disease [10,11], Lewy body dementia [12], and in familial and sporadic FTLD [5,13–16]. Some cross-sectional studies have suggested that cortical degeneration can be detected with MRI years before symptom onset in asymptomatic *MAPT* mutation carriers [5,14,17–19], but others have not shown any significant cortical volumetric differences between *MAPT* mutation carriers and controls [7,20]. Recently, two longitudinal studies from a cohort of asymptomatic *MAPT* mutation carriers have found atrophy in the hippocampus but no cortical atrophy was reported in longitudinal analysis during up to 4 years of follow-up [21,22]. Up to date, little is known about the trajectory of progression of atrophy on longitudinal MRI in asymptomatic *MAPT* mutation carriers.

In this study, we investigated the rates and trajectories of lobar atrophy on longitudinal MRI from asymptomatic stage to symptomatic stage in *MAPT* mutation carriers.

2. Methods

2.1. Participants

Participants in this study were enrolled in the Mayo Clinic Alzheimer's Disease Research Center and the Longitudinal Evaluation of Familial Frontotemporal Dementia Subjects (LEFFTDS) studies at the Mayo Clinic site. LEFFTDS is a multisite study investigating the biomarkers of disease progression in familial FTLD mutation carriers. The present study included participants who screened positive for a mutation in *MAPT* and had been followed up between August 2006 and November 2018 at Mayo Clinic. Participants with *MAPT* mutations who had no clinical symptoms at baseline and underwent at least two follow-up evaluations were included (n = 14). Noncarriers from healthy first-degree relatives of the patients were included as the control group after DNA screening (n = 13). All participants were followed up

prospectively with annual clinical examination at the time of MR examination, including a medical history review, mental status examination, a neurological examination by a clinician with FTLD expertise, and a neuropsychological examination. Participants were followed for a median of 9.2 years (range 2.0 to 11.7 years) and had at least 3 MRI scans, with a total of 166 MRI examinations. Of the 14 *MAPT* mutation carriers, 4 of them, all from a pallido-ponto-nigral degeneration (PPND) family with N279 K mutation [23], transitioned from asymptomatic stage to symptomatic stage during follow-up, which we refer to as converters. All converters were classified as MCI at the time of conversion, with two later developing features of mixed behavioral variant frontotemporal dementia and progressive supranuclear palsy (Richardson's syndrome), one developing behavioral variant frontotemporal dementia with parkinsonism and the other remaining MCI. The median age of symptom onset was 43.5 years with a range of 37–47 years, and the median follow-up interval was 9.7 years (range 8.7–11.7 years) for these four converters (typical for this PPND family). The remaining 10 *MAPT* mutation carriers (from 5 families) had no cognitive/behavioral/motor changes, which was corroborated by their informants and had an MMSE score of 30 throughout the median follow-up interval of 8.5 years (range 2.0–10.7 years), which we refer to as asymptomatic *MAPT* mutation carriers. The noncarriers did not differ from the asymptomatic *MAPT* mutation carriers and the converters on MMSE and DRS at baseline. The behavioral neurologist (B.F.B) who examined all the participants was blinded to the mutation status of all asymptomatic individuals regardless of mutation carrier status. None of the participants had structural lesions that could cause cognitive impairment or dementia, such as cortical infarction, subdural hematoma, or tumor, or had concurrent illness that would interfere with cognitive function other than FTLD on baseline and follow-up examinations.

All converters described in this report have undergone clinical genetic testing and therefore they and their proxies, as well as the examining neurologist, are aware of their mutation status. Most of the asymptomatic mutation carriers included in this report have not undergone clinical genetic testing and are therefore not aware of their mutation status. Details regarding each person have intentionally been excluded to maintain confidentiality.

Informed consent was obtained from all participants for participation in the studies, and after the three converters developed dementia, written assent was also obtained by their proxies. All procedures were approved by the Mayo Institutional Review Board.

2.2. MRI acquisition and process

All participants had volumetric MRI performed annually at 3T using an 8-channel phased array head coil (GE Healthcare, Milwaukee, WI) with a standard protocol. A 3D high-resolution T1-weighted magnetization-prepared rapid acquisition gradient echo (MPRAGE) was performed at each time point using following parameters: repetition time/echo time/inversion time = 2300/3/900 ms, flip angle 8°, in-plane resolution of 1.0 mm.

2.3. Region-level analysis

Baseline and annual changes in cortical volume were estimated for each participant. For the region-level analysis, we applied a fully automated in-house developed image-processing pipeline, using tensor-based morphometry with symmetric normalization (TBM-SyN) to compute the baseline lobar cortical volumes and changes over time in each participant [24]. For each participant, all their T1 structural MRI scans were iteratively coregistered to a mean image using a 6 degrees-of-freedom (6-DOF), followed by 9-DOF rigid body registration using SPM coregistration software [25] (www.fil.ion.ucl.ac.uk/spm). Then image intensity histograms across each participant's time series of images were normalized using an in-house developed differential bias correction algorithm [26]. The SyN diffeomorphic registration algorithm from ANTs software [26] was used to compute deformations between each pair of images, running the deformations explicitly in each direction, producing the Jacobian determinant images, and the "annualized" log of the Jacobian determinant from the deformation in each direction, to be parcellated into lobar regions of interest later. The voxel values of the Jacobian determinant image represent the expansion or contraction of each voxel over time, and those of the annualized log Jacobian determinant image can be thought of as analogous to an annualized percent change at each voxel. The SyN deformations were applied in each direction, respectively to the original bias corrected late and early images, to get the early image warped to the late, and the late image warped to the early image, and average them with their respective originals, resulting in a "synthetic late image" and a "synthetic early image." We then segmented the synthetic early and late images into gray matter, white matter, and cerebrospinal fluid classes using SPM with our in-house developed template [27]. The discrete cosine deformations from the unified segmentation step were used to transform the in-house modified AAL atlas that included the frontal, temporal, parietal, and occipital region of interest labels from template space to the synthetic early and late image spaces, respectively [28].

2.4. Voxel-level analysis

To assess the rates of atrophy at the voxel level, we used only the first and last images for each participant and ran the TBM-SyN steps as detailed previously to produce an image of the annualized log of the Jacobian determinant over the largest possible time interval for each participant. These images were smoothed with a 6 mm full-width at half maximum Gaussian smoothing kernel.

2.5. Genetic analysis

Participants recruited into this study are part of known *MAPT* families. For each of the participants, we specifically sequence the exon harboring the known *MAPT* mutation observed in that family using previously published protocol [29]. Sequencing is also performed to detect variants in the following genes *GRN, C9ORF72, TARDBP, PSEN1, PSEN2, and APP* according to the LEFFTDS protocol. PCR amplicons were purified using the Multiscreen system (Millipore, Billerica, MA) and then sequenced in both directions using Big Dye chemistry following the manufacturer's protocol (Applied Biosystems, Foster City, CA). Sequence products were purified using the Montage system (Millipore) before being run on an Applied Biosystem 3730 DNA Analyzer. Sequence data were analyzed using either SeqScape (Applied Biosystem) or Sequencher software (Gene Codes, Ann Arbor, MI).

2.6. Statistical analysis

Baseline characteristics of converters with *MAPT* mutations were described with means, standard deviations, counts, and proportions. Baseline characteristics were compared among converters, asymptomatic *MAPT* mutation carriers and noncarriers using generalized linear mixed models (categorical variables), or linear mixed models (continuous variables), adjusting for age where appropriate and accounting for the family structure using random effects. Tukey contrasts were subsequently used for pairwise comparisons.

Assessments of voxel-level results were corrected for multiple comparisons by requiring the corrected false discovery rate (FDR) to be < 0.05 and the uncorrected $P < .001$.

We modeled the log of lobar cortical volumes to estimate rate of volume loss expressed as percentage per year using linear mixed-effect models with random intercepts to account for within-subject repeated-measures correlations nested in within-family correlations. This allowed for dependence in the repeated measures per subject and also dependence in family members. Families were assumed to be independent from each other. Because of the sample size restrictions, we were only able to use random intercepts in these models. Inclusion of random slopes and flex points would result in gross overfitting of the models and nonconvergence. We coded group (noncarriers, asymptomatic, or converter) using dummy variables with noncarrier as the reference and included two-way interactions for group $\times$ age at MRI scan. Because we were interested in specific individual lobar cortical volume change hypotheses and not a universal null hypothesis and did not want to inflate the probability of a type II error, we did not adjust for multiple comparisons in these analyses.

3. Results

The baseline characteristics of the converters, asymptomatic *MAPT* mutation carriers, and noncarriers are shown in Table 1. There were no differences between the 3 groups at baseline based on sex, education, age at initial MRI scan, and cognitive scores. The converters had more MRI scans compared to asymptomatic *MAPT* mutation carriers ($P < .001$) and noncarriers ($P < .001$), but there were no differences in follow-up time range among the 3 groups. At baseline, temporal and frontal lobe volumes were lower in converters compared to asymptomatic *MAPT* mutation carriers ($P < .001$) and noncarriers ($P < .001$). Similarly, parietal lobe volumes were also lower in converters compared to asymptomatic *MAPT* mutation carriers ($P < .001$) and noncarriers ($P < .001$). No significant difference in lobar volume was observed between asymptomatic *MAPT* mutation carriers and noncarriers at baseline.

Fig. 1 shows the trajectories of change in lobar cortical volumes. The results of linear mixed-effects models are summarized in Table 2. Group $\times$ age at MRI scan interactions indicated that the converters had greater estimated annual rate of cortical atrophy in temporal ($P < .001$), frontal ($P < .01$), and parietal ($P < .05$) lobes compared to noncarriers. Similarly, the asymptomatic *MAPT* mutation carriers also had higher estimated annual rate of cortical atrophy in the temporal lobe than noncarriers ($P < .01$), but not in the frontal and parietal lobes. There was no difference in the estimated annual rate of occipital lobe cortical volume change among the 3 groups.

Voxel-based analysis showed that the annualized rate of atrophy was localized to the bilateral anterior and medial temporal lobe, inferior frontal lobe, limbic cortex, cingulate gyrus, precuneus, precentral gyrus, as well as the supplementary motor areas in all *MAPT* mutation carriers compared to noncarriers (corrected FDR <0.05) (Fig. 2). Because the *MAPT* mutation carriers also included four converters with N279 K mutation carriers from the same PPND family, we performed voxel-based analysis after removing the converters. Greater atrophy rates were found in the bilateral anterior and medial temporal lobe and orbitofrontal cortex in asymptomatic *MAPT* mutation carriers compared to noncarriers excluding the four converters ($P < .001$, not corrected for multiple comparisons).

4. Discussion

In this longitudinal study using 166 serial MRI scans, we report regional rates of atrophy in *MAPT* mutation carriers from the asymptomatic stage, four of whom became symptomatic during follow-up. In converters who became symptomatic during follow-up, we found that cortical atrophy was already present at baseline in the temporal, frontal, and parietal lobes, although they were asymptomatic at that time. On the other hand, no differences in lobar volumes were observed in asymptomatic *MAPT* mutation

Table 1
Baseline characteristics of participants and lobar cortical volumes

	Noncarrier (N = 13)	Asymptomatic (N = 10)	Converter (N = 4)	*P* value
No. female (%)	7 (54)	4 (40)	2 (50)	.95
Education, year	16 (2)	17 (3)	15 (3)	.34
Age at MRI scan, yr	36 (12)	31 (5)	39 (3)	.21
MMSE	30 (1)	30 (0)	30 (0)	.17
DRS total MOANS	12 (2)	11 (2)	12 (1)	.90
AVLT delay recalled MOANS	12 (4)	11 (2)	14 (1)	.82
No. of MRI scans	5 (2)	5 (2)	11 (2)	<.001*
Follow-up, yr	8 (3)	7 (3)	10 (1)	.49
Cortical volume at baseline (cm^3)				
Frontal	138 (8)	142 (18)	106 (11)	.001*
Temporal	117 (7)	126 (12)	85 (7)	<.001*
Parietal	70 (7)	71 (5)	53 (2)	<.001*
Occipital	64 (8)	65 (6)	53 (2)	.09

NOTE. Data shown are n (%) or mean (SD).

P values are from linear mixed models adjusting for age at MRI, also accounting for within-family correlations, followed by Tukey contrasts for pairwise comparisons.

Abbreviations: MRI, magnetic resonance imaging; MMSE, Mini–Mental State Examination; DRS, Dementia Rating Scale; MOANS, Mayo's Older Americans Normative Studies; AVLT, Auditory-Verbal Learning Test.

*Converter is statistically different from other groups.

carriers at baseline, who remained asymptomatic during follow-up compared to noncarriers. Our longitudinal data showed that the trajectories of lobar cortical atrophy were fastest in the temporal lobe, followed by frontal and parietal lobes in converters compared to noncarriers as they aged. The asymptomatic *MAPT* mutation carriers also showed a faster rate of temporal lobe cortical atrophy than noncarriers. Taken together, our cross-sectional and longitudinal findings demonstrated a sequential pattern of lobar atrophy in *MAPT* mutation carriers throughout the disease course, indicating that the temporal lobe cortical volume began declining during the asymptomatic stage, with an acceleration of the rates of atrophy during development of symptoms, followed by the involvement of the frontal and parietal lobes and sparing of the occipital lobe.

The temporal lobe cortical volumes declined in *MAPT* mutation carriers as early as the asymptomatic stage particularly in the bilateral medial temporal lobe on voxel-based analysis. This pattern is consistent with findings from previous cross-sectional MRI studies that demonstrate most prominent atrophy in the anteromedial temporal lobe and orbitofrontal cortex in asymptomatic *MAPT* mutation carriers [5,14,17]; however, others found no difference between asymptomatic *MAPT* mutation carriers and controls [7,20]. Gray matter decline in the hippocampus in asymptomatic *MAPT* mutation carriers was found in a recent longitudinal voxel-based morphometry study during 2 years of follow-up [21]. Another study reported extensive gray matter volume loss mainly in temporal and frontal lobes in a converter group combining 5 *MAPT* mutation and 3 *GRN* mutation carriers but found no longitudinal gray matter volume loss in asymptomatic *MAPT and GRN* mutation carriers who did not convert compared with noncarriers [22]. In the present study, we found lower baseline temporal lobe cortical volumes in converters, who later became symptomatic during follow-up compared to noncarriers. On the contrary, in the asymptomatic *MAPT* mutation carriers who remained asymptomatic, the temporal lobe cortical volumes were not different form noncarriers at baseline on cross-sectional analysis. The discordance in the literature on temporal lobe atrophy in asymptomatic *MAPT* mutation carriers may be due to the differences in the proximity to the age of symptom onset in cross-sectional studies of different asymptomatic *MAPT* mutation carrier cohorts or the sensitivity of the image analysis algorithm to relatively small amount of change in gray matter volume.

Early and accelerated rates of atrophy in the temporal lobe is a consistent finding in symptomatic carriers of *MAPT* mutations [13,16], suggesting that brain structural changes continue to occur in the same set of regions that are affected early in the disease. In keeping with that, the greatest atrophy rates were observed in the temporal lobe cortex in asymptomatic *MAPT* mutation carriers compared to noncarriers, which accelerated in those who became symptomatic. Given the increasing number of studies demonstrating early temporal atrophy in *MAPT* mutation carriers [13–16], our findings confirm and extend those reports and demonstrate early involvement of temporal lobe cortical atrophy in a longitudinal study design.

In the present study, the finding that frontal lobes especially the orbitofrontal lobe cortex present starting from the asymptomatic stage only in converters compared to noncarriers and became more atrophic as the disease progressed is consistent with atrophy patterns reported in previous voxel-based morphometry studies of familial FTD [5]. The progressive involvement of the frontal lobes followed the involvement of the temporal lobes, and the motor cortices, including the primary and supplementary motor cortices, were also affected in the asymptomatic *MAPT* mutation carriers on voxel-based analysis. However,

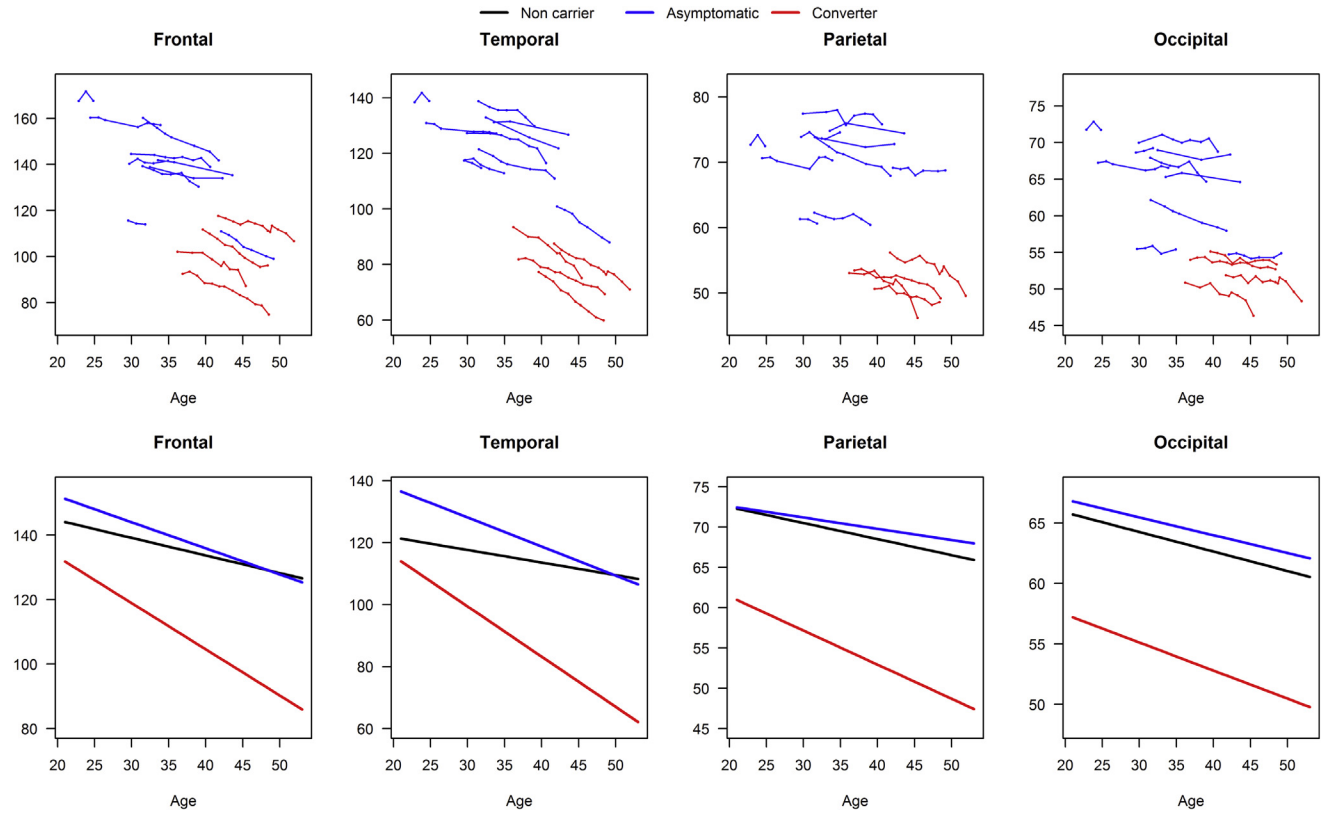

Fig. 1. Lobar volume plotted against age at MRI. Data point trajectories for individual *MAPT* mutation carriers (top panel) and the predicted volumes (cm^3) from the mixed models for each group (bottom panel) are shown. The blue line represents for the asymptomatic group who remained asymptomatic during the course of the study; the red line represents for the asymptomatic *MAPT* mutation carriers who converted; the black line represents the noncarriers. The noncarriers are not plotted in the top panel to show the data from the *MAPT* mutation carriers with clarity. Abbreviations: MAPT, microtubule-associated protein tau; MRI, magnetic resonance imaging.

greater rates of atrophy in the primary and supplementary motor cortices in *MAPT* mutation carriers compared to noncarriers were no longer statistically significant after removing the converters with *MAPT* N279K mutations who became symptomatic during follow-up from the voxel-based analysis. Patients with *MAPT* N279K mutations have prominent motor symptoms early in the disease process [23,30,31], and therefore, involvement of the primary and supplementary motor cortices may be expected in this group, influencing the results of the voxel-based analysis [32–36]. In symptomatic *MAPT* mutation carriers, the frontal lobes were reported to have the fastest rates of atrophy, followed by the temporal and parietal lobes [37]. Taken together with our findings, the temporal progression of lobar atrophy may follow a sequential pattern in *MAPT* mutation carriers. Temporal lobe cortical atrophy

Table 2
Predicted annual change in lobar volumes from mixed-effects models with noncarriers as the reference group

	Frontal	Temporal	Parietal	Occipital
	Estimates (95% CI)	Estimates (95% CI)	Estimates (95% CI)	Estimates (95% CI)
Intercept	155.5 (144.3, 166.8)*	129.8 (121.8, 137.8)*	76.5 (71.5, 81.5)*	69.1 (65.0, 73.2)*
Age at MRI scan	−0.55 (−0.82, −0.27)*	−0.41 (−0.62, −0.19)*	−0.20 (−0.29, −0.10)*	−0.16 (−0.24, −0.09)*
Asymptomatic	12.8 (−5.23, 30.7)	26.4 (13.6, 39.2)*	−1.10 (−8.62, 6.42)	0.77 (−5.74, 7.29)
Converter	6.37 (−17.0, 29.8)	18.2 (1.66, 34.8)†	−6.63 (−17.0, 3.75)	−7.03 (−15.6, 1.54)
Asymptomatic × age at MRI scan	−0.26 (−0.69, 0.16)	−0.53 (−0.86, −0.20)‡	0.06 (−0.09, 0.21)	0.01 (−0.10, 0.13)
Converter × age at MRI scan	−0.89 (−1.41, −0.36)‡	−1.21 (−1.63, −0.80)*	−0.22 (−0.40, −0.05)†	−0.07 (−0.21, 0.07)

NOTE. The noncarrier group regression equations contain the intercept and age at MRI terms. The asymptotic group equations add the "asymptotic" and "asymptotic × age at MRI scan" terms to the equation. The converter group equations instead add the "converter" and "converter × age at MRI scan" terms to the equation. These produce the predicted lines in Fig. 1. Because of the interactions in the models, age and group coefficients are not directly interpretable.

Abbreviations: CI, confidence interval; MRI, magnetic resonance imaging.

*$P < .001$.

†$P < .05$.

‡$P < .01$.

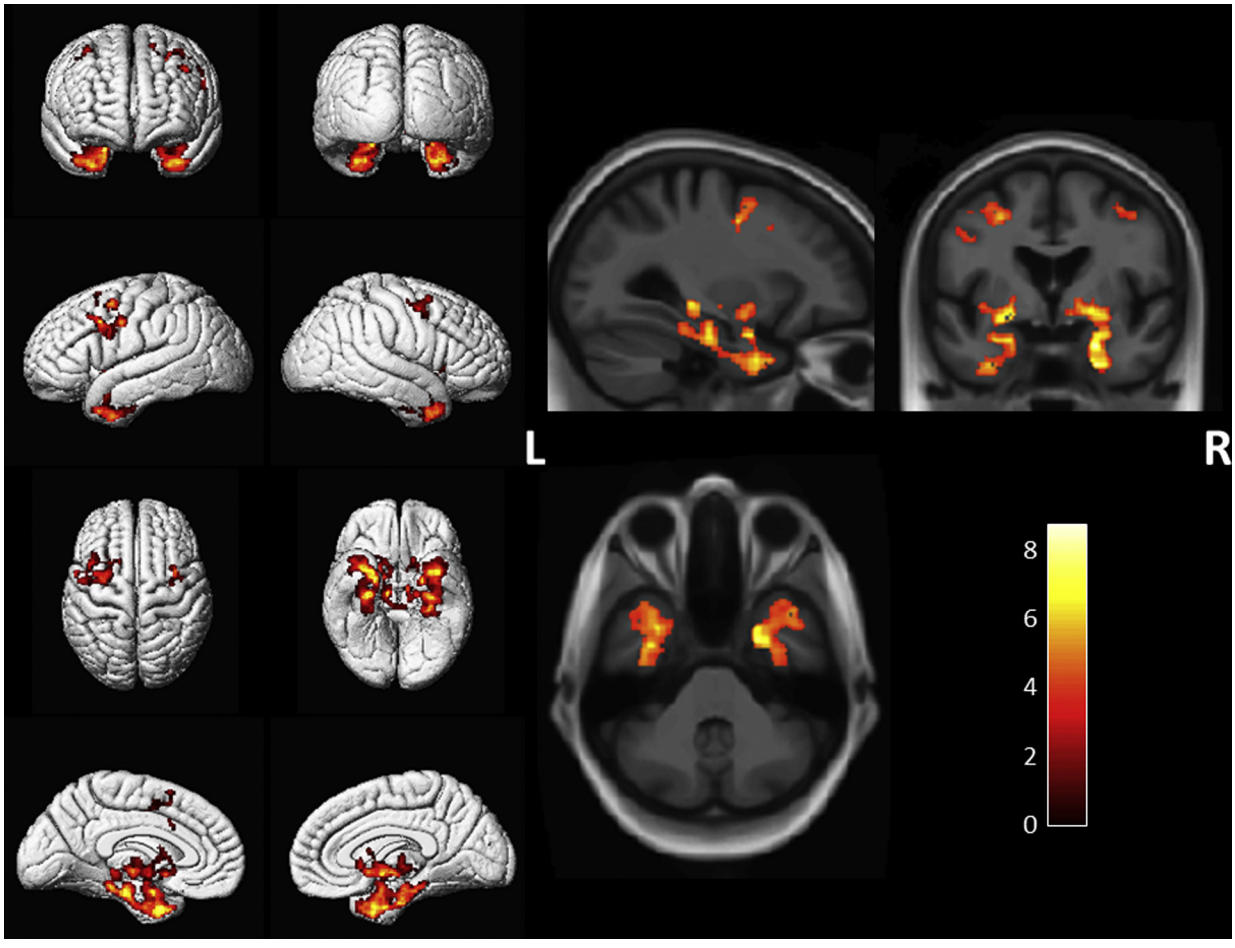

Fig. 2. Voxel-based analysis showed greater annualized rates of cortical atrophy in all *MAPT* mutation carriers compared to noncarriers. The results are shown at $P < .05$ after using the false discovery rate correction for multiple comparisons. Abbreviation: MAPT, microtubule-associated protein tau.

occurs in the earliest stages during the asymptomatic stage. After the patients become symptomatic, the rates of atrophy may slow down in the temporal lobes but accelerates in the frontal lobes during the later stages of disease progression.

Our data showed that parietal lobe cortical atrophy, especially in the precuneus, was present starting from the asymptomatic stage only in converters compared to noncarriers, but with relatively slower rates of atrophy than the temporal and frontal lobes. However, the rates of cortical atrophy in the parietal lobe were not different from asymptomatic *MAPT* mutation carriers compared to noncarriers. Thus, the parietal lobe cortical atrophy occurred later than temporal lobe involvement, but also years before symptom onset when asymptomatic *MAPT* mutation carriers approaching closely to the symptom onset age, and progressed slower than temporal and frontal lobe cortical atrophy. This pattern of parietal cortical lobe atrophy is consistent with findings reported in symptomatic *MAPT* mutation carriers [15]. The early involvement of parietal lobe was also found in an ^{1}H MR spectroscopy study that demonstrated early metabolite abnormalities in the posterior cingulate and precuneus cortex in asymptomatic *MAPT* mutation carriers [6]. Similarly, mild glucose hypometabolism in the parietal lobes on PET was found in N279K *MAPT* mutation carriers from the same PPND family, along with ballooned neurons and abundant tau inclusions in the parietal cortex at autopsy [33]. The early involvement of the parietal lobe cortex, particularly the paralimbic regions such as the precuneus, but a relatively slow progression of atrophy in this region may be associated with the gradual involvement of limbic pathways that connect the anteromedial temporal lobe to the medial parietal cortex in patients with *MAPT* mutations who are approaching the symptomatic stage [38,39].

One strength of our study was the large number of serial MRIs collected over 10 years and tracking of the disease progression from asymptomatic to symptomatic stage; however, the relatively small number of participants in each group was still a limitation. Although one of our previous cross-sectional studies had shown similar patterns atrophy across different submutation types in *MAPT* mutation carriers [16], there may be variability in the rates of atrophy within the asymptomatic *MAPT* mutation carriers across different specific mutations. Subtypes of *MAPT* mutation have been shown to cause different types of tauopathies. These are mutations inside exon 10 (i.e., N279K, P301L, and S305N) that tend

to form four tandem microtubule-binding domain repeat (4R-tau) pathology relative to 3 repeat (3R tau) pathology [40], and mutations outside exon 10 (i.e., V337M and R406W) that tend to form mixed 3 R/4R tau pathology. The 4 converters in the present study all had N279K *MAPT* mutations, and their trajectories of lobar atrophy, such as the supplemental motor cortex involvement, may be specific to the suspected 4R-tau-associated neurodegeneration in N279K kindreds. Further studies are needed to characterize the trajectories of rates of brain atrophy across the different *MAPT* mutations.

In summary, our data indicate a sequential pattern of regional cortical atrophy rates involving the temporal lobe cortex early on, followed by the frontal and parietal lobe cortices in *MAPT* mutation carriers as they transition from asymptomatic stage to symptomatic stage. Our findings support the clinical utility of using longitudinal regional volumes for monitoring the neurodegenerative disease progression in *MAPT* mutation carriers starting from the asymptomatic stage. Lobar cortical atrophy rates may also have a utility in clinical trials involving agents that potentially modify neurodegenerative disease pathology in asymptomatic *MAPT* mutation carriers.

Acknowledgments

The authors extend their appreciation to the staff of all centers and particularly to their patients and their families for their participation in this protocol.
This work is supported by NIH grants U01 AG045390, U54 NS092089, U24 AG021886, U01 AG016976, and R01 AG 40042.

RESEARCH IN CONTEXT

1. Systematic review: The authors reviewed the literature using traditional (e.g., PubMed) sources and meeting abstracts and presentations.
2. Interpretation: Our findings provide details on a sequential pattern of regional cortical atrophy rates in microtubule-associated protein tau (*MAPT*) mutation carriers as they transition from asymptomatic stage to symptomatic stage.
3. Future directions: The manuscript proposes a framework of using longitudinal regional volumes for monitoring the neurodegenerative disease progression in *MAPT* mutation carriers starting from the asymptomatic stage. Further studies are needed to characterize the trajectories of rates of brain atrophy across the different subtypes of *MAPT* mutation.

References

[1] Bang J, Spina S, Miller BL. Frontotemporal dementia. Lancet 2015; 386:1672–82.
[2] Rohrer JD, Warren JD. Phenotypic signatures of genetic frontotemporal dementia. Curr Opin Neurol 2011;24:542–9.
[3] Ingram EM, Spillantini MG. Tau gene mutations: dissecting the pathogenesis of FTDP-17. Trends Mol Med 2002;8:555–62.
[4] Bunker JM, Kamath K, Wilson L, Jordan MA, Feinstein SC. FTDP-17 mutations compromise the ability of tau to regulate microtubule dynamics in cells. J Biol Chem 2006;281:11856–63.
[5] Cash DM, Bocchetta M, Thomas DL, Dick KM, van Swieten JC, Borroni B, et al. Patterns of gray matter atrophy in genetic frontotemporal dementia: results from the GENFI study. Neurobiol Aging 2018; 62:191–6.
[6] Kantarci K, Boeve BF, Wszolek ZK, Rademakers R, Whitwell JL, Baker MC, et al. MRS in presymptomatic MAPT mutation carriers: a potential biomarker for tau-mediated pathology. Neurology 2010; 75:771–8.
[7] Dopper EG, Rombouts SA, Jiskoot LC, den Heijer T, de Graaf JR, de Koning I, et al. Structural and functional brain connectivity in presymptomatic familial frontotemporal dementia. Neurology 2014; 83:e19–26.
[8] Vemuri P, Weigand SD, Knopman DS, Kantarci K, Boeve BF, Petersen RC, et al. Time-to-event voxel-based techniques to assess regional atrophy associated with MCI risk of progression to AD. Neuroimage 2011;54:985–91.
[9] Whitwell JL, Petersen RC, Negash S, Weigand SD, Kantarci K, Ivnik RJ, et al. Patterns of atrophy differ among specific subtypes of mild cognitive impairment. Arch Neurol 2007;64:1130–8.
[10] Risacher SL, Anderson WH, Charil A, Castelluccio PF, Shcherbinin S, Saykin AJ, et al. Alzheimer disease brain atrophy subtypes are associated with cognition and rate of decline. Neurology 2017;89:2176–86.
[11] Cash DM, Ridgway GR, Liang Y, Ryan NS, Kinnunen KM, Yeatman T, et al. The pattern of atrophy in familial Alzheimer disease: volumetric MRI results from the DIAN study. Neurology 2013; 81:1425–33.
[12] Murray ME, Ferman TJ, Boeve BF, Przybelski SA, Lesnick TG, Liesinger AM, et al. MRI and pathology of REM sleep behavior disorder in dementia with Lewy bodies. Neurology 2013;81:1681–9.
[13] Rohrer JD, Ridgway GR, Modat M, Ourselin S, Mead S, Fox NC, et al. Distinct profiles of brain atrophy in frontotemporal lobar degeneration caused by progranulin and tau mutations. Neuroimage 2010;53:1070–6.
[14] Fumagalli GG, Basilico P, Arighi A, Bocchetta M, Dick KM, Cash DM, et al. Distinct patterns of brain atrophy in Genetic Frontotemporal Dementia Initiative (GENFI) cohort revealed by visual rating scales. Alzheimers Res Ther 2018;10:46.
[15] Whitwell JL, Jack CR Jr, Boeve BF, Senjem ML, Baker M, Rademakers R, et al. Voxel-based morphometry patterns of atrophy in FTLD with mutations in MAPT or PGRN. Neurology 2009; 72:813–20.
[16] Whitwell JL, Jack CR Jr, Boeve BF, Senjem ML, Baker M, Ivnik RJ, et al. Atrophy patterns in IVS10+16, IVS10+3, N279K, S305N, P301L, and V337M MAPT mutations. Neurology 2009;73:1058–65.
[17] Rohrer JD, Nicholas JM, Cash DM, van Swieten J, Dopper E, Jiskoot L, et al. Presymptomatic cognitive and neuroanatomical changes in genetic frontotemporal dementia in the Genetic Frontotemporal dementia Initiative (GENFI) study: a cross-sectional analysis. Lancet Neurol 2015;14:253–62.
[18] Spina S, Farlow MR, Unverzagt FW, Kareken DA, Murrell JR, Fraser G, et al. The tauopathy associated with mutation +3 in intron 10 of Tau: characterization of the MSTD family. Brain 2008; 131:72–89.
[19] Cordes M, Wszolek Z, Calne D, Rodnitzky RL, Pfeiffer RF. Magnetic resonance imaging studies in rapidly progressive autosomal dominant

parkinsonism and dementia with pallido-ponto-nigral degeneration. Neurodegeneration 1992;1:217–24.
[20] Whitwell JL, Josephs KA, Avula R, Tosakulwong N, Weigand SD, Senjem ML, et al. Altered functional connectivity in asymptomatic MAPT subjects: a comparison to bvFTD. Neurology 2011;77:866–74.
[21] Panman JL, Jiskoot LC, Bouts M, Meeter LHH, van der Ende EL, Poos JM, et al. Gray and white matter changes in presymptomatic genetic frontotemporal dementia: a longitudinal MRI study. Neurobiol Aging 2019;76:115–24.
[22] Jiskoot LC, Panman JL, Meeter LH, Dopper EGP, Donker Kaat L, Franzen S, et al. Longitudinal multimodal MRI as prognostic and diagnostic biomarker in presymptomatic familial frontotemporal dementia. Brain 2019;142:193–208.
[23] Wszolek ZK, Pfeiffer RF, Bhatt MH, Schelper RL, Cordes M, Snow BJ, et al. Rapidly progressive autosomal dominant parkinsonism and dementia with pallido-ponto-nigral degeneration. Ann Neurol 1992;32:312–20.
[24] Cash DM, Frost C, Iheme LO, Unay D, Kandemir M, Fripp J, et al. Assessing atrophy measurement techniques in dementia: Results from the MIRIAD atrophy challenge. Neuroimage 2015;123:149–64.
[25] Ashburner J, Friston KJ. Unified segmentation. Neuroimage 2005; 26:839–51.
[26] Avants BB, Epstein CL, Grossman M, Gee JC. Symmetric diffeomorphic image registration with cross-correlation: evaluating automated labeling of elderly and neurodegenerative brain. Med Image Anal 2008;12:26–41.
[27] Vemuri P, Whitwell JL, Kantarci K, Josephs KA, Parisi JE, Shiung MS, et al. Antemortem MRI based STructural Abnormality iNDex (STAND)-scores correlate with postmortem Braak neurofibrillary tangle stage. Neuroimage 2008;42:559–67.
[28] Tzourio-Mazoyer N, Landeau B, Papathanassiou D, Crivello F, Etard O, Delcroix N, et al. Automated anatomical labeling of activations in SPM using a macroscopic anatomical parcellation of the MNI MRI single-subject brain. Neuroimage 2002;15:273–89.
[29] Hutton M, Lendon CL, Rizzu P, Baker M, Froelich S, Houlden H, et al. Association of missense and 5'-splice-site mutations in tau with the inherited dementia FTDP-17. Nature 1998;393:702–5.
[30] Wszolek ZK, Kardon RH, Wolters EC, Pfeiffer RF. Frontotemporal dementia and parkinsonism linked to chromosome 17 (FTDP-17): PPND family. A longitudinal videotape demonstration. Mov Disord 2001;16:756–60.
[31] Wszolek ZK, Tsuboi Y, Uitti RJ, Reed L. Two brothers with frontotemporal dementia and parkinsonism with an N279K mutation of the tau gene. Neurology 2000;55:1939.
[32] Arima K, Kowalska A, Hasegawa M, Mukoyama M, Watanabe R, Kawai M, et al. Two brothers with frontotemporal dementia and parkinsonism with an N279K mutation of the tau gene. Neurology 2000;54:1787–95.
[33] Arvanitakis Z, Witte RJ, Dickson DW, Tsuboi Y, Uitti RJ, Slowinski J, et al. Clinical-pathologic study of biomarkers in FTDP-17 (PPND family with N279K tau mutation). Parkinsonism Relat Disord 2007; 13:230–9.
[34] Cheshire WP, Tsuboi Y, Wszolek ZK. Physiologic assessment of autonomic dysfunction in pallidopontonigral degeneration with N279K mutation in the tau gene on chromosome 17. Auton Neurosci 2002; 102:71–7.
[35] Ferman TJ, McRae CA, Arvanitakis Z, Tsuboi Y, Vo A, Wszolek ZK. Early and pre-symptomatic neuropsychological dysfunction in the PPND family with the N279K tau mutation. Parkinsonism Relat Disord 2003;9:265–70.
[36] Slowinski J, Dominik J, Uitti RJ, Ahmed Z, Dickson DD, Wszolek ZK. Frontotemporal dementia and Parkinsonism linked to chromosome 17 with the N279K tau mutation. Neuropathology 2007;27:73–80.
[37] Whitwell JL, Boeve BF, Weigand SD, Senjem ML, Gunter JL, Baker MC, et al. Brain atrophy over time in genetic and sporadic frontotemporal dementia: a study of 198 serial magnetic resonance images. Eur J Neurol 2015;22:745–52.
[38] Mahoney CJ, Simpson IJ, Nicholas JM, Fletcher PD, Downey LE, Golden HL, et al. Longitudinal diffusion tensor imaging in frontotemporal dementia. Ann Neurol 2015;77:33–46.
[39] Elahi FM, Marx G, Cobigo Y, Staffaroni AM, Kornak J, Tosun D, et al. Longitudinal white matter change in frontotemporal dementia subtypes and sporadic late onset Alzheimer's disease. Neuroimage Clin 2017;16:595–603.
[40] McCarthy A, Lonergan R, Olszewska DA, O'Dowd S, Cummins G, Magennis B, et al. Closing the tau loop: the missing tau mutation. Brain 2015;138:3100–9.